INTERNATIONAL JOURNAL OF CONSERVATION SCIENCE

ISSN: 2067-533X Volume 16, Issue 3, 2025: 1597-1610 www.ijcs.ro

DOI: 10. 36868/IJCS.2025.03.25

# REMOTE SENSING AND GIS APPLICATION IN SURFACE WATER QUALITY RESEARCH IN THE CHEPINSKA RIVER BASIN (WESTERN RHODOPES, BULGARIA)

Emilia TCHERKEZOVA[1*], Kalin MARKOV[1], Marian VARBANOV[2], Elitsa ZAREVA[3]

[1] National Institute of Geophysics, Geodesy and Geography, Bulgarian Academy of Sciences – Division of Applied Geoinformatics at Geography Department, Acad. G. Bonchev Str. 3, Sofia, Bulgaria, 1113,
[2] National Institute of Geophysics, Geodesy and Geography, Bulgarian Academy of Sciences – Hydrology and Water Management Research Center, Acad. G. Bonchev Str. 3, Sofia, Bulgaria, 1113,
[3] University of Mining and Geology "St. Ivan Rilski", Department of Geology and Geoinformatics, Prof. Boyan Kamenov Str. 1, Sofia, Bulgaria, 1700

***Abstract***

*Unlike traditional water sampling methods for surface water quality analysis and assessment, satellite imagery has good spatial and temporal coverage, allowing analysis of large areas. In this work, we used satellite data from the Copernicus Sentinel-2 satellite mission, a digital elevation model (DEM), and GIS techniques and methods to extract water bodies in the Chepinska River Basin (Western Rhodopes). The obtained results were analyzed together with the water quality analysis results of in situ measurements and surface water samples, data from the Executive Environmental Agency of the Ministry of Environment and Water, the Ministry of Agriculture, Food, and Forestry, Bulgaria, and high-resolution Global Surface Water Datasets (1984- 2021). The integrated GIS-based analysis allowed us to determine the extent of water bodies in different years and seasons, the degree of surface water pollution, and the points for long-term monitoring of river water quality in the investigated area. The obtained results are also useful for improving the quality of existing data sets available from other sources, such as the East Aegean River Basin Directorate (Plovdiv), and for supporting the Chepinska River basin management.*

***Keywords****: Copernicus Sentinel-2 satellite mission; GIS; Global Surface Water Datasets (1984-2021); Surface water quality; Chepinska River Basin; Western Rhodopes*

## Introduction

The rapid development of geoinformation technologies over the past decades provides an opportunity to integrate Geographic Information Systems (GIS) and remote sensing methods and techniques with traditional methods for surface water quality assessment at a river basin scale. The main advantages of such methodological approaches in natural sciences are the good spatial and temporal coverage of satellite imagery and the low-cost possibilities for the identification of water bodies, channels, and wetlands, as well as for water quality monitoring over large areas, such as drainage basins. Over the past decades, various methods for delineation of water bodies and wetland areas using remote sensing images from Landsat and Sentinel 2 missions have been used, for example: i) *index-based methods*: Normalized Difference Water Index (NDWI) [1], Land surface water index (LSWI) [2], modified Normalized Difference Water Index (MNDWI) [3], Water Ratio Index (WRI) [4], Red Edge NDWI [5], Automated Water Extraction Index

* Corresponding author: emivat2017@gmail.com

(AWEIsh and AWEInsh) [6], Sentinel Water Mask (SWM) [7], New Water Index (NWI) [8], Moisture Stress Index (MSI) [9], Sentinel-2 Water Index (SWI) with Otsu method [10], Triangle Water Index (TWI) [11]; ii) *various machine learning algorithms* such as artificial neural networks (ANN) [12, 13], Support vector machines (SVM) [14], Random Forest (RF) [15], and iii) *classification methods*, e.g. maximum likelihoods (MLs) [16], and decision trees (DTs), e.g. [17]. Index-based methods specialize in the detection of water bodies using the spectral characteristics and differences of different features in each band, or using multi-band inter-spectral analysis methods [18], and then thresholding based on reflectivity differences among the water bodies and other surface features [19, 20]. Classification and machine learning algorithm methods require high professional knowledge and experience, which restricts their use, especially in mountainous regions, where there are sources of noise such as clouds, shadows, and snow [18, 20].

Since inland surface water bodies are important components of the hydrosphere and inland water ecosystems, water quality monitoring and assessment are critical for river basin management. In this work, we present the results of GIS techniques and methods using remote sensing data from the Copernicus Sentinel-2 satellite mission, surface water quality data obtained through traditional water sampling methods and analysis from the Executive Environmental Agency of the Bulgarian Ministry of Environment and Water (ExEA-MOEW), our own surface water sample points, as well as data from the Bulgarian Ministry of Agriculture, Food, and Forestry, and a high-resolution Global Surface Dataset (1984-2021) [21, 32].

The obtained water bodies and channels are useful for improving the quality of existing data sets available from other sources, such as the East Aegean River Basin Directorate (Plovdiv).

The integrated analysis allowed us to determine the degree of surface water pollution and the most suitable locations for long-term monitoring of the river water quality in the Chepinska River Basin (Western Rhodope Mountains, Bulgaria).

## Materials and Methods

### *Study Area and Data*

The Chepinska River is one of the major tributaries on the right bank of the Maritsa River, stretching 81.7 km in length (Fig. 1). It springs from the Batashka Mountains (Western Rhodopes, Bulgaria) at an altitude of 1990m a.s.l. From its spring the river flows to the northeast and then west-northwest, until a forested location called Karatepe. Then it continues flowing through a deep and wooded valley under the name Chepinska (Banska Bistrica) River. In the southern part of the city of Velingrad, the river enters the Chepinska Hollow. This part of the river flows through a wide valley. This is also the location where it receives its largest tributary, the Matnitsa River. After that, the Chepinska River circles the northern side of Lakatina Chuka Peak (1058.9m a.s.l.) and then makes a southeast turn. Near the village of Draginovo, it leaves the valley, cutting into the Chepinski Gorge between Alabak Hill in the northwest and Karkaria in the southeast, initially flowing north, then southeast, and finally northeast, before flowing into the Maritsa River.

The drainage basin of the study area covers a region of around 977.6km$^2$, according to the data obtained from the East Aegean River Basin Directorate (Decision No ZDOI-01-86(2) from 24$^{th}$ July 2023).

It is part of the Moravian-Rhodope zone and more specifically in the Rila-Rhodope tectonic unit (parts of the Western Rhodopes zone) [22]. According to those authors and the geological maps with a scale of 1:100 000 (map sheet Velingrad [23], map sheet Rakitovo [24], map sheet Pazardzhik [25], and map sheet Razlog [26] the area is geologically heterogeneous. It contains Precambrian high-grade metamorphic rocks, intrusive igneous rocks (mainly Paleozoic medium-grained biotite granites and Late Cretaceous aplitoid-pegmatoid granites), and Neogene

and Quaternary sediments of alluvial, deluvial, proluvial character – boulders, gravels, sands, clays.

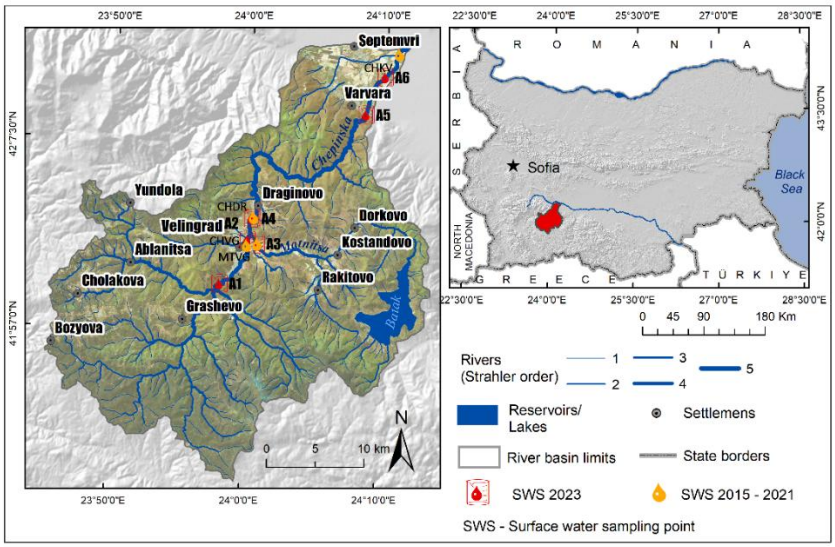


**Fig. 1.** Location of the study area and surface water sampling points

The climate of the Chepinska River Basin is transitional continental with a mild winter one, a small annual amplitude of air temperature, two minimums (August and February), and two maximums (July and November) of precipitations [27].

The study area belongs to the Pazardzhik District with the following municipalities: Velingrad, Rakitovo, Batak, and Septemvri [28, 29, 30].

Table 1 shows the data sets used in this study.

**Table 1.** Data sets used in this study

| | Data | Data type/ spatial resolution |
|---|---|---|
| 1 | Copernicus Sentinel-2 Collection 1 MSI Level-2A (L2A) from 2022-05-20, cloud cover 0.006, S2A_MSIL2A_20220520T090601_N0400_R050_T35TKG_20220520T135214.SAFE | Raster, 10m |
| 2 | Copernicus Sentinel-2 Collection 1 MSI Level-1C (L1C) from 2022-11-01, cloud cover 0, S2B_MSIL1C_20221101T091029_N0400_R050_T35TKG_20221101T100434.SAFE | Raster, 10m |
| 3 | Digital Terrain Model (DTM) for Continental Europe [31] | Raster, 30 m, resampled |
| 4 | Land use (physical blocks). Date: 2024, Ministry of Agriculture and Food (MAF) [21]. [Online], Available: https://cadis.bg/2024/03/29/ | Vector |
| 5 | Global Surface Water dataset [32] | Raster, 10 m |
| 6 | Data from East Aegean River Basin Directorate (Plovdiv) (Decisions No ZDOI-01-86(2) from 24th July 2023 and No ZDOI-01-116(1) from 11th Nov 2023) | Vector |
| 7 | Open Street Map Project (OSM): settlements, roads, railroads. [44]. [Online], Available: https://download.geofabrik.de/europe/bulgaria.html | Vector |
| 8 | Data from Executive Environment Agency (Ministry of Environment and Water), [Online], Available: https://earbd.bg/indexdetails.php?menu_id=609 | Vector |
| 9 | Water sampling from selected in this study monitoring points during a field campaign in the Summer of 2023 | GPS and shape data |

Sentinel-2 Level-1C provides a Top-Of-Atmosphere (TOA) corrected surface reflectance product. The Level-2A product is a Bottom-Of-Atmosphere (BOA) reflectance product. It includes a scene classification (including Clouds and Cloud Shadows), AOT (Aerosol Optical Thickness), WV (Water Vapour) maps) (European Space Agency, 2024. https://sentiwiki.copernicus.eu/web/s2-products).

***Methods***

First, BOA atmospheric correction was performed for the Sentinel 2A Level 1C data product using the Sentinel Application Platform (SNAP, http://step.esa.int/).

In the next step, the following water and vegetation indices were calculated to extract water bodies using the Sentinel-2A satellite data, in a QGIS environment (Table 2).

**Table 2**. Remotely sensed water and vegetation indices calculated in this study

| Water indices | Equation | Source |
|---|---|---|
| NDWI | [(Green − NIR) / (Green + NIR)] | [1] |
| MNDWI | [(Green − SWIR) / (Green + SWIR)] | [3] |
| Re_NDWI | [(Green − NIR) / (Green + NIR)] | [5] |
| CEDEX | (NIR / RED) − (NIR / SWIR) | cited by [33] |
| $AWEI_{sh}$ | Blue + 2.5 * Green − 1.5 * (NIR + SWIR) − 0.25 − SWIR | [6] |
| $AWEIn_{sh}$ | 4 * (Green − NIR) − (0.25 * NIR + 2.75 * SWIR) | [6] |
| B-BLUE | (Blue − NIR) / (Blue + NIR) | [33] |
| LSWI | NIR − SWIR1) / (NIR + SWIR1) | [2]) |
| MSI | SWIR1 / NIR | [9] |
| SWI | (Red edge − SWIR 1)/(Red edge + SWIR 1) | [10] |
| SWM | (Blue + Green) / (NIR + SWIR 1) | [7]) |
| WRI | (Green + Red) / (NIR + SWIR) | [4] |
| NDVI | (NIR − Red) / ( NIR + Red) | [34] |

Following the calculation of the water indices, the Pearson correlation coefficient between them was calculated (Tables 3 and 4).

Using the obtained results, thresholds were defined for each water index using the QGIS plugin “Thresholds to ROI”. The results were then vectorized and water bodies were outlined.

Another approach used to delineate water bodies was the Mean Shift Segmentation (MSS) method, which identifies water bodies using a clustering technique, without needing labeled training data. In this case, the band combination B11-B05-B02 was used.

To verify the accuracy of the water body indices, NDVI [34], and the Mean Shift Segmentation classification, 800 random points were generated using ArcGIS and then classified as water (1) and non-water (0) using Google Earth (Google LLC) and the Sentinel−2 band combination B11-B05-B02 [18, 34].

The Digital Terrain Model [31] was resampled to a grid size of 10 m using additional elevation information. This model was used for digital terrain analysis to obtain stream networks, sub-basins, and hydrologically relevant geomorphometric variables and indices.

In this study, we also applied the Canadian Water Quality Index [35]. This index is a comprehensive tool used to assess the overall health of water bodies by summarizing data from various individual water quality measurements. This index can be used to model the anthropogenic impact on water bodies based on their physicochemical parameters or quality elements. It is determined using three main factors: Scope (F1), which measures the percentage of parameters measured that fail to meet water quality guidelines; Frequency (F2), which indicates the percentage of individual tests made that do not meet these guidelines; and Amplitude (F3), which assesses the extent of deviation of failing tests from the guidelines. By integrating these factors into a single index score, the CCME WQI provides an accessible overview of water quality, ranging from excellent to poor, and helps identify areas needing attention or improvement.

$$CCME\ WQI = 100 - \left( \frac{\sqrt{F_1^2 + F_2^2 + F_3^2}}{1{,}732} \right) \quad (1)$$

The divisor 1.732 normalizes the obtained value so that it is in the interval from 0 to 100, where 0 means "worst quality", and 100 – "best quality" of water. The CCME-WQI applied model also offers the following differentiation of the water quality status into categories: ***excellent*** (WQI = 95–100), ***good*** (WQI = 80–94), ***fair*** (WQI = 65–79), ***marginal*** (WQI = 45–64), ***poor*** (WQI = 0–44) [34, 35].

## Results and discussion

Figure 2 shows the calculated water indices on the example of the Sentinel-2 image from 1st November 2022.

The overall correlation between the calculated water and vegetation indices is represented in Tables 3 and 4. For the Sentinel-2 (L1C) image from 2022-11-01, the best correlation exists between the water indices SWM and WRI (0.993), followed by MNDWI and SWI (0.978), B-Blue and NDWI (0.970), and $AWEI_{nsh}$ and $AWEI_{sh}$ (0.937) (Sentinel – 2A, Date: 2022-11-01) (Table 3).

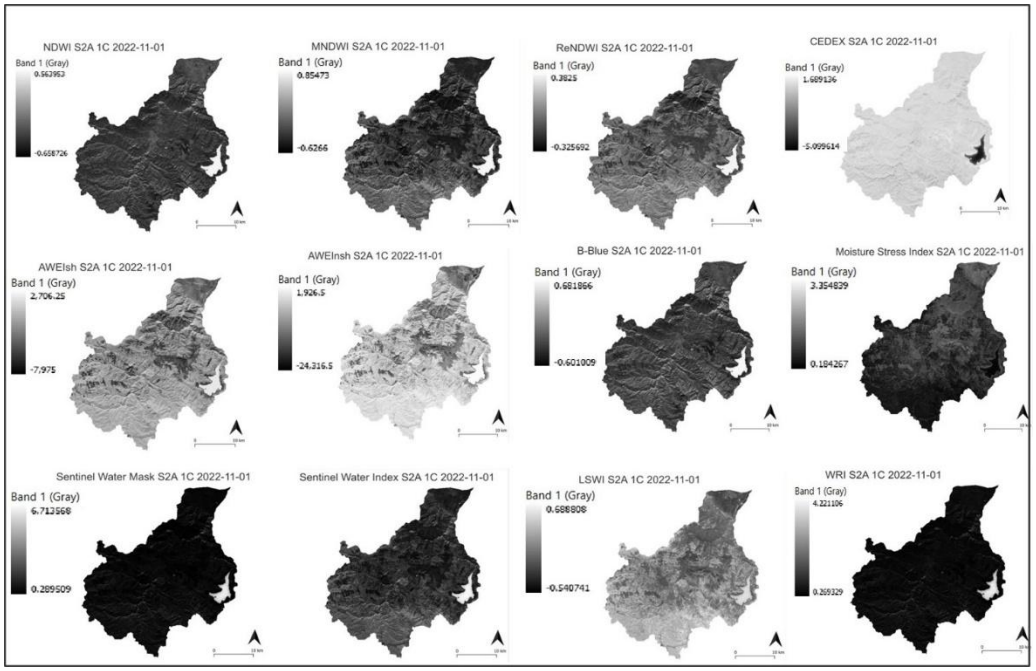


**Fig. 2.** Water indices obtained from Sentinel-2A image (Date: 2022-11-01)

The best correlation for the satellite image Sentinel-2 (L2A), date: 2022-05-20 is between the following vegetation indices: B-Blue and NDWI (0.991), followed by SWM and WRI (0.987), B-Blue and WRI (0.977), NDWI and NDVI (0.977), NDWI and WRI (0.976), and B-Blue and NDVI (0.976) (Table 4).

**Table 3.** Pearson correlation matrix of the calculated water indices and NDVI (Sentinel-2 Collection 1 MSI Level-1C, 2022-11-01)

| Pearson correlation matrix (Sentinel-2 Collection 1 MSI Level-1C, 2022-11-01) | | | | | | | | | | | | | |
|---|---|---|---|---|---|---|---|---|---|---|---|---|---|
| * | **1** | **2** | **3** | **4** | **5** | **6** | **7** | **8** | **9** | **10** | **11** | **12** | **13** |
| **1** | 1.000 | | | | | | | | | | | | |
| **2** | 0.937 | 1.000 | | | | | | | | | | | |
| **3** | 0.499 | 0.726 | 1.000 | | | | | | | | | | |
| **4** | -0.39 | -0.512 | -0.737 | 1.000 | | | | | | | | | |
| **5** | 0.793 | 0.622 | 0.138 | -0.402 | 1.000 | | | | | | | | |
| **6** | 0.817 | 0.851 | 0.713 | -0.765 | 0.781 | 1.000 | | | | | | | |
| **7** | -0.80 | -0.613 | -0.103 | 0.348 | -0.982 | -0.736 | 1.000 | | | | | | |
| **8** | 0.331 | 0.582 | 0.970 | -0.785 | 0.030 | 0.640 | 0.011 | 1.000 | | | | | |
| **9** | 0.833 | 0.879 | 0.712 | -0.707 | 0.737 | 0.961 | -0.704 | 0.629 | 1.000 | | | | |
| **10** | 0.757 | 0.786 | 0.699 | -0.815 | 0.759 | 0.978 | -0.709 | 0.640 | 0.890 | 1.000 | | | |
| **11** | 0.430 | 0.548 | 0.810 | -0.955 | 0.351 | 0.759 | -0.308 | 0.849 | 0.696 | 0.817 | 1.000 | | |
| **12** | 0.349 | 0.486 | 0.798 | -0.961 | 0.273 | 0.705 | -0.230 | 0.860 | 0.643 | 0.768 | 0.993 | 1.000 | |
| **13** | -0.18 | 0.108 | 0.713 | -0.599 | -0.439 | 0.167 | 0.475 | 0.827 | 0.156 | 0.208 | 0.609 | 0.609 | 1.000 |

* 1 – $AWEI_{nsh}$, 2-$AWEI_{sh}$, 3-B-Blue, 4-CEDEX, 5-LSWI, 6-MNDWI, 7-MSI, 8-NDWI, 9-Re-NDWI, 10-SWI, 11-SWM, 12-WRI, 13-NDVI

**Table 4.** Pearson correlation matrix of the calculated water indices and NDVI (Sentinel-2 Collection 1 MSI Level-2A, 2022-05-20)

| Pearson correlation matrix of (Sentinel-2 Collection 1 MSI Level-2A, 2022-05-20) | | | | | | | | | | | | | |
|---|---|---|---|---|---|---|---|---|---|---|---|---|---|
| * | **1** | **2** | **3** | **4** | **5** | **6** | **7** | **8** | **9** | **10** | **11** | **12** | **13** |
| **1** | 1.000 | | | | | | | | | | | | |
| **2** | -0.83 | 1.000 | | | | | | | | | | | |
| **3** | 0.242 | -0.529 | 1.000 | | | | | | | | | | |
| **4** | -0.34 | 0.556 | -0.896 | 1.000 | | | | | | | | | |
| **5** | 0.289 | 0.164 | -0.807 | 0.636 | 1.000 | | | | | | | | |
| **6** | 0.783 | -0.639 | 0.596 | -0.657 | -0.035 | 1.000 | | | | | | | |
| **7** | -0.34 | -0.104 | 0.790 | -0.607 | -0.989 | 0.018 | 1.000 | | | | | | |
| **8** | 0.205 | -0.482 | 0.991 | -0.872 | -0.820 | 0.596 | 0.806 | 1.000 | | | | | |
| **9** | 0.498 | -0.480 | 0.683 | -0.732 | -0.281 | 0.755 | 0.270 | 0.667 | 1.000 | | | | |
| **10** | 0.759 | -0.562 | 0.345 | -0.403 | 0.162 | 0.876 | -0.179 | 0.357 | 0.347 | 1.000 | | | |
| **11** | 0.434 | -0.596 | 0.952 | -0.853 | -0.613 | 0.777 | 0.597 | 0.945 | 0.783 | 0.529 | 1.000 | | |
| **12** | 0.328 | -0.528 | 0.977 | -0.891 | -0.698 | 0.718 | 0.685 | 0.976 | 0.749 | 0.469 | 0.987 | 1.000 | |
| **13** | 0.076 | -0.403 | 0.976 | -0.895 | -0.881 | 04759 | 0.870 | 0.977 | 0.595 | 0.238 | 0.880 | 0.938 | 1.000 |

* 1 – $AWEI_{nsh}$, 2-$AWEI_{sh}$, 3-B-Blue, 4-CEDEX, 5-LSWI, 6-MNDWI, 7-MSI, 8-NDWI, 9-Re-NDWI, 10-SWI, 11-SWM, 12-WRI, 13-NDVI

The threshold values (t) for each water and vegetation index were determined for water bodies delineation using the QGIS Plugin "Threshold to ROI". Based on those thresholds water bodies were identified (Figs. 3 and 4).

We also tried the Mean Shift Segmentation algorithm using the B11-B05-B02 bands to delineate the water bodies in the study area without the need of having training data. The MSS is a clustering method that clusters an image by associating each pixel with a peak of the image's probability density function [37]. According to these authors, "this peak is computed by defining a window in the pixel neighborhood and then calculating the mean of the pixels within the window, and then the window is shifted to the mean, and similar steps are repeated until convergence". The result of the mean shift is only controlled by the kernel size (bandwidth) and therefore requires less manual intervention than other algorithms [37].

The obtained results were then vectorized. Visual analysis showed that all indices with the selected threshold values recognise different patterns. Some of them, such as AWEIsh, AWEInsh, LSWI, and MSI extracted not only pure water pixels, but also made classification errors such as

recognising hilly shadows, built-up areas, and bare land as water areas. The best results were delivered using the defined threshold values of NDWI, SWI, SWM, and WRI indices, as well as the Mean Shift Segmentation classification.

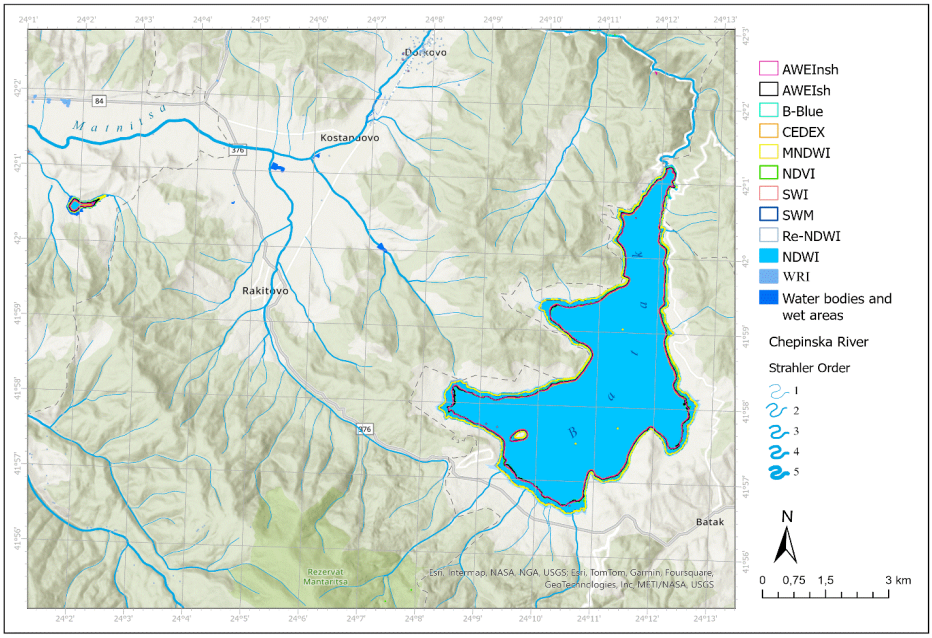


**Fig. 3.** An example of the water body limits of Batak and Matnitsa Reservoirs delineated through the threshold method from water indices and open data from the Ministry of Agriculture, Food, and Forestry, Bulgaria

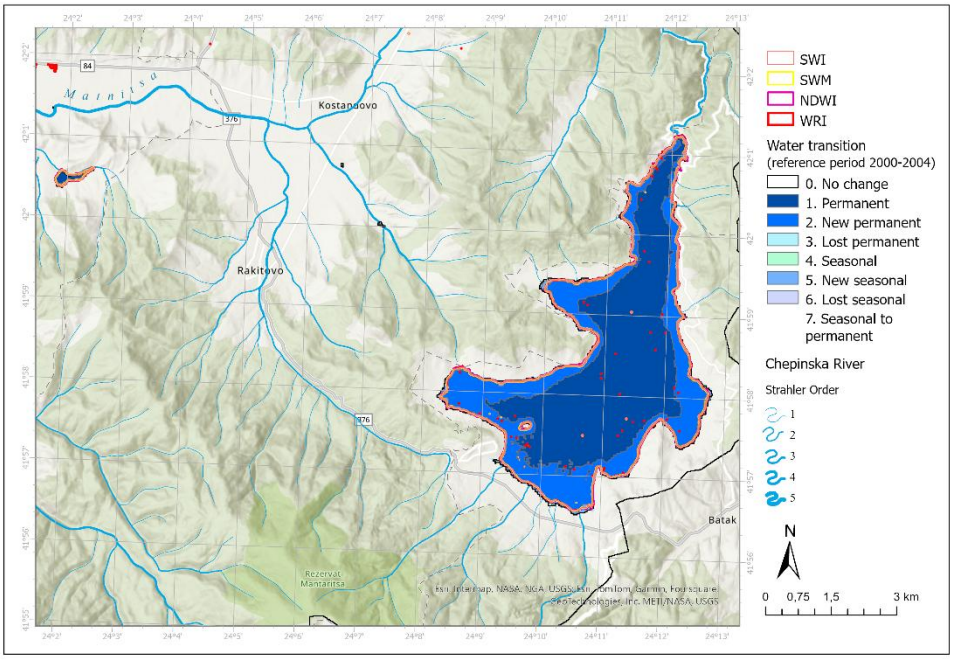


**Fig. 4.** An example of the water body boundaries of Batak and Matnitsa Reservoirs delineated through the threshold method from water indices and open data from high-resolution Global Surface Data (reference period 1984-2021)

The non-water areas were then removed manually using the band composite B11-B05-B02 and the classified Mean Shift Segmentation layer.

Figures 3 and 4 show the water body limits obtained by employing the different methods and post-processing steps used in this study, as well as those from the Ministry of Agriculture and Forestry and the high-resolution Global Surface Water Data (Table 1).

Table 5 represents the area (in $km^2$) of the Batak and Matnitsa Reservoirs obtained using the above-described methods.

The difference in the areas and water volumes of the Batak and Matnitsa Reservoirs is attributed to the different water indices used and the different seasons in which the imagery was obtained (20 May and 1 November 2022). Among the performed methods, the results from Mean Shift Segmentation using the band composite B11-B05-B02 (Sentinel−2, date 2011-11-01) and from the thresholded indices produce the best overall accuracy (OA). For the Batak reservoir, the following thresholded indices performed best: NDWI (OA - 0.9683), SWI (OA - 0.9634), SWM (OA - 0.9612), and WRI (OA - 0.9467).

**Table 5.** Waterbody limits of Batak and Matnitsa Reservoirs obtained by employing different methods

| | | **Sentinel 2A, 2022-11-01** | | **Sentinel 2A, 2022-05-20** | |
|---|---|---|---|---|---|
| | | **Batak ($km^2$)** | **Matnitsa ($km^2$)** | **Batak ($km^2$)** | **Matnitsa ($km^2$)** |
| 1 | **AWEInsh** | 16.64 | 0.07 | 19.61 | 0.14 |
| 2 | **AWEIsh** | 16.80 | 0.09 | 19.61 | 0.14 |
| 3 | **B-Blue** | 16.94 | 0.10 | 19.20 | 0.14 |
| 4 | **CEDEX** | 16.50 | 0.05 | 19.35 | 0.13 |
| 5 | **LSWI** | 16.37 | 0.06 | 15.48 | 0.14 |
| 6 | **MDWI** | 16.66 | 0.06 | 19.20 | 0.13 |
| 7 | **MSI** | 16.30 | 0.08 | 15.46 | 0.14 |
| 8 | **NDWI** | 19.02 | 0.12 | 19.42 | 0.14 |
| 9 | **ReNDWI** | 19.16 | 0.13 | 19.17 | 0.13 |
| 10 | **SWI** | 18.83 | 0.13 | 19.10 | 0.13 |
| 11 | **SWM** | 18.82 | 0.13 | 19.10 | 0.13 |
| 12 | **WRI** | 18.75 | 0.13 | 19.32 | 0.14 |
| 13 | **NDVI** | 17.05 | 0.13 | 14.77 | 0.14 |
| 14 | **Mean Shift Segmentation (band combination 11-05-02)** | 19.06 | 0.13 | 19.10 | 0.14 |
| 15 | **Water and wetland*** | 20.77 | 0.23 | 20.77 | 0.23 |

* Data from the Ministry of Agriculture, Food, and Forestry, Bulgaria

The following hydro-morphological descriptors were obtained using digital terrain analysis (DTA): stream networks (length, Strahler order), drainage basins, and sub-basins (area, perimeter, and drainage density), as well as slope and aspect (in degrees) and the Melton Ruggedness Number [38]. For this study, the river metrics are of greatest interest. The total length of the stream networks, including ephemeral streams and gullies, is 100.51km. River segments with Strahler order 4 and 5 have lengths of 34.2 and 45.30km, respectively.

The quality status of the Chepinska River is determined by applying the Canadian Water Quality Index (CCME WQI), developed for the needs of the Ministry of the Environment of Canada and widely used in many countries, including Bulgaria [39, 40]. The water quality assessment of the river was carried out according to the normative requirements of Regulation N-

4 [41, 42] according to ten approved chemical indicators. The obtained annual results and the average values of the CCME WQI index for the period 2015-2021 in four monitoring points for water quality do not meet the reference values for “good chemical status”, according to the requirements of the Regulation. Using the original CCME WQI rating scale, the average values of the index at the selected monitoring locations define the quality of the river water as "critical" or "poor". The quality of the water of Matnitsa and Chepinska rivers in the Velingrad region is bad and critical – both before the city and downstream, before its confluence with the Maritsa River (Table 6 and Figure 5).

The causes, sources, and forms of pollution have been reviewed and discussed in a previous article [43].

Table 6. Water quality according to the CCME WQI

| Sample points | Sample point A2 (Figure 6) | | | Sample point A3 (Figure 6) | | | Sample point 2 (Figure 6) | | | Sample point A6 (Figure 6) | | |
|---|---|---|---|---|---|---|---|---|---|---|---|---|
| Indicators | **mean** | maximum | minimum | **mean** | maximum | minimum | **mean** | maximum | minimum | **mean** | maximum | minimum |
| **CCME WQI** | **57.8** | 67.2 | 30.9 | **36.2** | 41.6 | 31.9 | **36.1** | 45.7 | 29.5 | **59.5** | 48.61 | 14.9 |

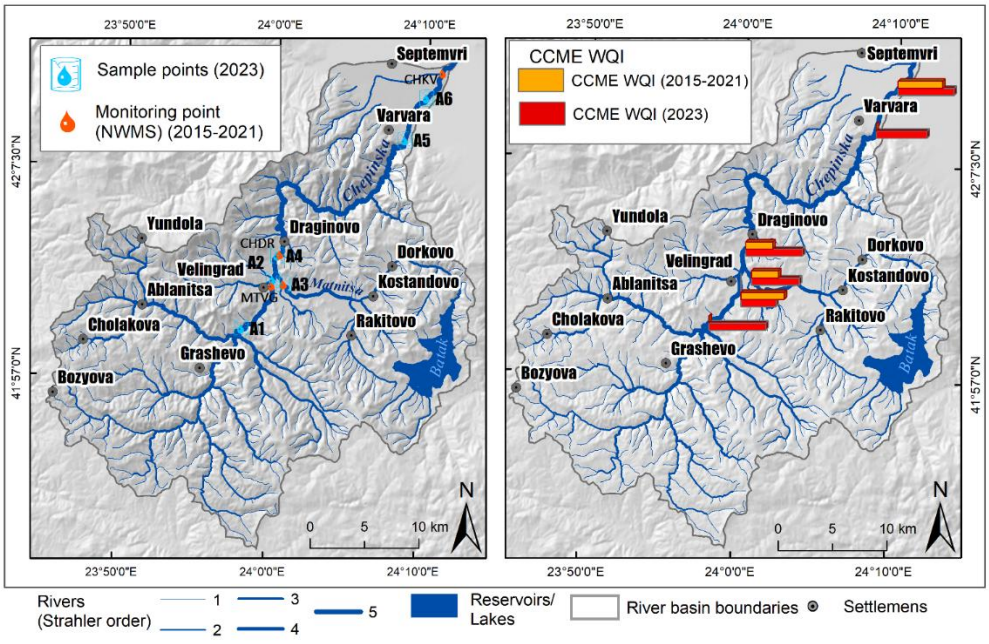


**Fig. 5.** Surface water quality according to the CCME WQI in the investigated monitoring points

Since the analysis of surface water quality and transformation of water resources is mainly done in rivers and reservoirs, the quality of spatial hydrographic and morphographic data is essential. Data from satellite images obtained at different times of the year, as well as digital terrain models with different spatial resolutions, enable fast and efficient research and tracking of changes in the size and quality of water bodies. The obtained results show that, in contrast to purely open and unobscured surface water bodies (large rivers and reservoirs) in other studies (mentioned in the introduction of this article), the identification and extraction of surface water

in areas such as the Chepinska River catchment is difficult due to dense forest vegetation in places. Also, there are problems with incorrect identification of waters in bare-earth and built-up areas from some remote sensing water indices. In this case, the employment of water indexes and NDVI should be explored together with data from other large-scale sources and field campaigns.

The results show that the calculated water indices have different sensitivities to different types of water bodies (e.g. in terms of size and depth).

Overall, the Mean Shift Segmentation method results are better than the threshold method used for water body delineation based on the calculated water indices and NDVI.

The analysis of surface water quality shows a medium and high level of surface water pollution, which should be monitored in the future. Because the higher values are in and around settlements and anthropogenic facilities, such as industrial and rural areas, it is recommended to extend the monitoring in the area between the Batak Dam and the mouth of the Matnitsa River, as well as in the lower reaches of the Chepinska River (Figures 1 and 5).

## Conclusions

In the Chepinska River Basin, (Western Rhodopes) Canadian WQI and statistical methods were used to assess the surface water quality in selected locations, which are the subject of the National Water Monitoring System (NWMS) for the period (2015-2021). We also performed our own field sampling in 2023. The integrated GIS-based analysis allowed us to determine the degree of surface water pollution at the points for long-term monitoring of the river water quality in the investigated area.

Unlike traditional water sampling methods for surface water quality analysis and assessment, satellite imagery has good spatial and temporal coverage, allowing analysis of large areas. That is why in this work, we also focused on the problem of how remote sensing and geoinformation technologies could contribute to the estimation of surface water characteristics and quality. Satellite data from the Copernicus Sentinel-2 satellite mission, a digital elevation model (DEM), and GIS techniques and methods were used to extract water bodies, stream networks, and sub-catchments. This was done by calculation of various water indexes and geomorphometric DEM-analysis. The results were compared with open waterbody data from the Ministry for Agriculture and Forestry, Bulgaria [21], and high-resolution Global Surface Water Datasets (1984-2021) from the Joint Research Center [32]. They show that the most appropriate method is the Mean Shift Segmentation, followed by the threshold values approach for the water indices NDWI, SWI, SWM, and WRI.

The integrated GIS-based analysis allowed us to determine the extent of water bodies in different years and seasons, the degree of surface water pollution, and the points for long-term monitoring of river water quality in the investigated area. The obtained results are also useful for improving the quality of existing data sets available from other sources, such as the East Aegean River Basin Directorate (Plovdiv), and for supporting the Chepinska River basin management.

## Acknowledgments

This research has been carried out in the frame of the project “Models of anthropogenic impact on the natural environment at river basin scale (ModAiNe)”, funded by the National Science Fund, Ministry of Education and Science (Bulgaria), Competition for financial support for basic research projects – 2022 (Contract No КП-06-Н64/6, signed on 15th December 2022).

The authors acknowledge the East Aegean River Basin Directorate (Plovdiv) for providing the hydrological data necessary for the study. The authors would like, also, to thank all anonymous reviewers for their constructive comments.

**References**

[1] S.K. McFeeters, *The use of the Normalized Difference Water Index (NDWI) in the Delineation of Open Water Features*, **International Journal of Remote Sensing**, **17**(7), 1996, pp. 1425–1432. DOI: 10.1080/01431169608948714.

[2] X. Xiao, S. Boles, S. Frolking, W. Salas, B. Moore, C. Li, R. Zhao, *Landscape-scale characterization of cropland in China using Vegetation and Landsat TM images*, **International Journal of Remote Sensing**, **23**(18), 2002, pp. 3579–3594. DOI: 10.1080/01431160110106069.

[3] H. Xu, *Modification of normalised difference water index (NDWI) to enhance open water features in remotely sensed imagery*, **International Journal of Remote Sensing**, **27**(14), 2006, pp. 3025–3033. DOI: 10.1080/01431160600589179.

[4] L. Shen, C. Li, *Water body extraction from Landsat ETM+ imagery using adaboost algorithm*. **18th International Conference on Geoinformatics. IEEE**, 2010, pp. 1–4.

[5] S. Klemenjak, B. Waske, S. Valero, J. Chanussot, *Unsupervised river detection in RapidEye data*. **Proceedings of the IEEE International Geoscience and Remote Sensing Symposium**, Munich, Germany, 22–27 July 2012, 2012, pp. 6860–6863.

[6] G.L. Feyisa, H. Meilby, R. Fensholt, S.R. Proud, *Automated Water Extraction Index: A new technique for surface water mapping using Landsat imagery*, **Remote Sensing of Environment**, **140**, 2014, pp. 23–35. DOI: 10.1016/j.rse.2013.08.029.

[7] A. Robak, A. Gadawska, M. Milczarek, S. Lewiński, *The detection of water on Sentinel-2 imagery based on water indices*, **Teledetekcja Środowiska, 55**(2), 2016, pp. 59-72. (In Polish, Abstract in Englisch)

[8] H. Tian, W. Li, M. Wu, N.I. Huang, G. Li, X. Li, Z. Niu, *Dynamic monitoring of the largest freshwater lake in China using a new water index derived from high spatiotemporal resolution Sentinel-1A data*. **Remote Sens., 9**(6), 2017, 521. https://doi.org/10.3390/rs9060521.

[9] R. Coluzzi, V. Imbrenda, M. Lanfredi, T. Simoniello, *A first assessment of the Sentinel-2 Level 1-C cloud mask product to support informed surface analyses*, **Remote Sensing of Environment, 217**, 2018, pp. 426-443. DOI: 10.1016/j.rse.2018.08.009.

[10] W. Jiang, Y. Ni, Z. Pang, G. He, J. Fu, J. Lu, K. Yang, T. Long, T. Lei, 2020. *A New Index for Identifying Water Body from Sentinel-2 Satellite Remote Sensing Imagery*. **ISPRS Annals of the Photogrammetry, Remote Sensing and Spatial Information Sciences**, **Volume V-3-2020**, XXIV ISPRS Congress (2020 edition), V-3-2020, 2020, pp. 33–38, https://doi.org/10.5194/isprs-annals-V-3-2020-33-2020, 2020.

[11] L. Niu, H. Kaufmann, G. Xu, G. Zhang, C. Ji, Y. He, M. Sun, *Triangle Water Index (TWI): An Advanced Approach for More Accurate Detection and Delineation of Water Surfaces in Sentinel-2 Data*. **Remote Sensing, 14**, 2022, Article Number: 5289. https://doi.org/10.3390/rs14215289.

[12] S. Skakun, *A neural network approach to flood mapping using satellite imagery*. **Comput. Inform.**, **29**, 2010, pp. 1013–1024.

[13] K. Rokni, A. Ahmad, K. Solaimani, S. Hazini, *A new approach for surface water change detection: Integration of pixel level image fusion and image classification techniques*,

**International Journal of Applied Earth Observation and Geoinformation, 34**, 2015, pp. 226–234. DOI: 10.1016/j.jag.2014.08.014.

[14] F. Sun, Y, Zhao, P. Gong, R. Ma, Y. Dai, *Monitoring dynamic changes of global land cover types: fluctuations of major lakes in China every 8 days during 2000–2010*, **Chinese Science Bulletin, 59**(2), 2014, pp. 171–189. DOI: 10.1007/s11434-013-0045-0.

[15] M. Belgiu, L. Drăguţ, *Random forest in remote sensing: A review of applications and future directions*. **ISPRS Journal Photogramm. Remote Sensing, 114**, 2016, pp. 24–31.

[16] J. Yang, X, Du, *An enhanced water index in extracting water bodies from Landsat TM imagery*, **Annals of GIS, 23**(3), 2017, pp. 141–148. DOI: 10.1080/19475683.2017.1340339.

[17] T.D. Acharya, D.H. Lee, D., I.T. Yang, J.K., Lee, *Identification of Water Bodies in a Landsat 8 OLI Image Using a J48 decision tree*, **Sensors, 16**(7), 2016, 1075. https://doi.org/10.3390/s16071075.

[18] Q. Sun, J. Li, *A method for extracting small water bodies based on DEM and remote sensing images*, **Scientic Report**, **14**, 2024, Article Number: 760, https://doi.org/10.1038/s41598-024-51346-7.

[19] T.D. Acharya, A. Subedi, A., D.H. Lee*, Evaluation of water indices for surface water extraction in a Landsat 8 scene of Nepal*, **Sensors 18**(8), 2018, Article Number: 2580. https://doi.org/10.3390/s18082580.

[20] H.W. Khalid, R.M.Z. Khalil, M.A. Qureshi, *Evaluating spectral indices for water bodies extraction in western Tibetan Plateau*, **Egyptian Journal of Remote Sensing and Space Science, 24**(3), 2021, pp. 619–634. DOI: 10.1016/j.ejrs.2021.09.003.

[21] Ministry of Agriculture and Food (MAF). Land use (physical blocks). Date: 2024 [Online]. Available: https://cadis.bg/2024/03/29/.

[22] H. Dabovski, I Zagorchev, *Alpine tectonic subdivision of Bulgaria*, **Geology of Bulgaria. Part II, Mesozoic Geology** (Editors: I. Zagorchev, H. Dabovski, T. Nikolov), "Prof. Marin Drinov" Publishing House, Sofia, 2009, pp. 30–37 (in Bulgarian, with English abstract).

[23] R. Dimitrova, N. Katskov, *Geological Map of Bulgaria, Scale 1:100 000, Velingrad Sheet.* **Committee of Geology, Deptment of Geophysical Prospecting and Geological Mapping,** Sofia, 1990. (in Bulgarian).

[24] D. Kozhoukharov, R. Dimitrova, N. Katskov, *Geological Map of Bulgaria, Scale 1:100 000, Rakitovo Sheet,* **Committee of Geology, Deptment of Geophysical Prospecting and Geological Mapping,** Sofia, 1990. (in Bulgarian).

[25] D. Kozhoukharov, R. Dimitrova, N. Katskov, *Geological Map of Bulgaria, Scale 1:100 000, Pazardzhik Sheet.* **Committee of Geology, Deptment of Geophysical Prospecting and Geological Mapping,** Sofia, 1990 (in Bulgarian).

[26] R. Marinova, N. Katskov, *Geological Map of Bulgaria, Scale 1:100 000, Razlog Sheet.* **Committee of Geology, Dept. of Geophysical Prospecting and Geological Mapping,** Sofia, 1990. (in Bulgarian).

[27] S. Velev, *Climatic zoning*. **Geography of Bulgaria. Physical geography and Socio-economic geography (**Editors: I. Kopralev, M. Yordanova, Ch. Mladenov), Publishing House ForCom, SOFIA, 2002, pp. 155-166.

[28] * * *, Integrated Development Plan of Velingrad Municipality, 2021-2027. [Online}. https://m.velingrad.bg/wp-content/uploads/2021/02/%D0%9F%D0%98%D0%A0%D0%9E-%D0%92%D0%95%D0%9B%D0%98%D0%9D%D0%93%D0%A0%D0%90%D0%94-2021-2027.pdf, Accessed on 15 August 2024.

[29] * * *, Integrated Development Plan of Rakitovo Municipality, 2021-2027. [Online]. https://www.strategy.bg/StrategicDocuments/View.aspx?lang=bg-BG&Id=1392, Accessed on 15 August 2024.

[30] * * *, Integrated Development Plan of Septemvri Municipality, 2021-2027. [Online]. https://www.strategy.bg/strategicdocuments/View.aspx?lang=bg-BG&Id=1481, Accessed on 15 August 2024.

[31] T. Hengl, L. Leal Parente, J. Krizan, B. Carmelo, *Continental Europe Digital Terrain Model at 30 m resolution based on GEDI, ICESat-2, AW3D, GLO-30, EUDEM, MERIT DEM and background layers (v0.3)* [Data set]. 2020, Zenodo. https://doi.org/10.5281/zenodo.4724549.

[32] * * *, Joint Research Centre. *Global Surface Water - Data Users Guide (v4)*. [Online]. [Accseden on 14th April 2024].

[33] J. Pena-Regueiro, M.-T. Sebastiá-Frasquet, J. Estornell, J.A. Aguilar-Maldonado, *Sentinel-2 Application to the Surface Characterization of Small Water Bodies in Wetlands*. **Water**, **12**, 2020, 1487. https://doi.org/10.3390/w12051487.

[34] U.S. Geological Survey. Landsat Normalized Difference Vegetation Index (NDVI)**.** [Online]. https://www.usgs.gov/landsat-missions/landsat-normalized-difference-vegetation-index, [Accessed on 10 January 2024].

[35] Canadian Council of Ministers of the Environment (CCME). Canadian water quality guidelines for the protection of aquatic life: Canadian Water Quality Index 1.0 Technical Report, 2017. [Online]. https://ccme.ca/en/res/wqimanualen.pdf, [Accessed on 24 April 2024].

[36] UNEP − United Nations Environment Programme. *Global Drinking Water Quality Index Development and Sensitivity Analysis Report*, UNEP: Toronto, ON, Canada, 2007; p. 60.

[37] H. Zhou, X Wang, G. Schaefer, *Chapter 13. Mean Shift and Its Application in Image Segmentation*. **Innovations in Intelligent Image Analysis**, (Editors: H. Kwásnicka, L.C. Jain, SCI 339, 2011, pp. 291–312.

[38] L. Marchi, G.D. Fontana, *GIS morphometric indicators for the analysis of sediment dynamics in mountain basins*. **Environmental Geology, 48**(2), 2005, pp. 218-228, DOI 10.1007/s00254-005-1292-4. DOI10.1007/s00254-005-1292-4.

[39] G. Yotova, M. Varbanov, E. Tcherkezova, St. Tsakovski, *Water quality assessment of a river catchment by the composite water quality index and self-organizing maps*, **Ecological Indicators, Volume 120**, Elsevier, 2021, https://doi.org/10.1016/j.ecolind.2020.106872, ISSN:1470-160X.

[40] K. Gartsiyanova, M. Varbanov, A. Kitev, St. Genchev, E. Tcherkezova, *Water Conservation and River Water Quality of the Bulgarian Black Sea Tributaries*. **International Journal of Conservation Science, 13(3)**, 2022, pp. 981-990.

[41] * * *, MOEW, Ministry of the environment and water - Regulation N-4/14.09.2012 for characterization of surface waters, Bulgaria, 2013. (In Bulgarian).

[42] * * *, MOEW (Ministry of Environment and Water) 2012. Ordinance No N-4 2012 about the characterisation of surface water. 54 p. (in Bulgarian), https://www.moew.government.bg/static/media/ups/tiny/filebase/Wa-ter/Legislation/Naredbi/NAREDBA_N-4_ot_14.09.2012_g._za_harakterizirane_na_ povarhnostnite_vodi.pdf. [Online]. [Accessed on 22 April 2023].

[43] M. Varbanov, K. Gartsiyanova, St. Genchev, G. Metodieva, *Assessment of the Chepinska River Waters Quality through the Combined Use of Different Indices*. DOI: 10.5593/sgem2023V/3.2/s12.05, **23rd SGEM International Multidisciplinary Scientific**

**GeoConference 2023. Conference Proceedings of selected papers. Water Resources, Forest, Marine and Ocean Ecosystems. Hydrology and Water Resources, Oil % Gas Exploration, Forest Ecosystems,** Vol. 23, Issue 3.2, STEF92 Technology, 2023, https://epslibrary.at/sgem_jresearch_publication_view.php?page=view&editid1=9390.

[44] Open Street Map Project (OSM): settlements, roads, railroads. [44]. [Online], Available: https://download.geofabrik.de/europe/bulgaria.html.

*Received: September 20, 2024*
*Accepted: June 28, 2025*